TITLE PAGE

Title

Detectability of regional lung ventilation with flat-panel detector-based dynamic radiography

Authors

Rie Tanaka, PhD [1]*
Shigeru Sanada, PhD [1]
Nobuo Okazaki, MD [2]
Takeshi Kobayashi, MD [3]
Masayuki Suzuki, MD [1]
Takeshi Matsui, RT [4]
Osamu Matsui, MD [4]

* Corresponding author

Affiliation

[1] Graduate School of Medical Science, Kanazawa University; 5-11-80 Kodatsuno, Kanazawa, 920-0942, Japan
[2] Department of Internal medicine, Ohtsuka Ryougoku Clinic; 2-4-10, Ryougoku, Sumidaku, Tokyo, 130-0026, Japan
[3] Department of Radiology, Ishikawa Prefectural Central Hospital; 2-1 Kuratsuki Higashi, Kanazawa, 920-8530, Japan
[4] Department of Radiology, Kanazawa University Hospital; 13-1 Takaramachi, kanazawa, 920-8642, Japan

Telephone and Fax numbers and e-mail address of Corresponding Author

R. Tanaka, PhD
Tel: +81-76-265-2537
Fax: +81-76-234-4366
E-mail: rie44@mhs.mp.kanazawa-u.ac.jp
Graduate School of Medical Science, Kanazawa University; 5-11-80 Kodatsuno, Kanazawa, 920-0942, Japan

Information concerning grants

This work was supported in part by Canon Inc. and a Grant-in-Aid for Scientific Research from the Japanese Ministry of Education, Culture, Sports, Science, and Technology: Intelligent Assistance in Diagnosis of Multi-dimensional Medical Images.

ABSTRACT

This study was performed to investigate the ability of breathing chest radiography using flat-panel detector (FPD) to quantify relative local ventilation. Dynamic chest radiographs during respiration were obtained using a modified FPD system. Imaging was performed in three different positions, *i.e.*, standing, and right and left decubitus positions, to change the distribution of local ventilation. We measured the average pixel value in the local lung area. Subsequently, the inter-frame differences as well as difference values between maximum inspiratory and expiratory phases were calculated. The results were visualized as images in the form of a color display to show more or less X-ray translucency. Temporal changes and spatial distribution of the results were then compared to lung physiology. In the results, the average pixel value in each lung was associated with respiratory phase. In all positions, respiratory changes of pixel value in the lower area was greater than that in the upper area ($P<0.01$), which was the same tendency as the regional differences in ventilation determined by respiratory physiology. In addition, in the decubitus position, it was observed that areas with large respiratory changes in pixel value moved up in the vertical direction during expiration, which was considered to be airway closure. In conclusion, breathing chest radiography using FPD was shown to be capable of quantifying relative ventilation in local lung area, and detecting regional differences in ventilation and timing of airway closure. This method is expected to be useful as a new diagnostic imaging modality for evaluating relative local ventilation.

Keywords: Digital Imaging, Functional Imaging, Computer Analysis, Chest Radiographs, flat-panel detector, FPD, ventilation

INTRODUCTION

Background

The lung vessels and bronchial volume per unit volume change dynamically due to respiration. These changes are reflected in respiratory changes in X-ray translucency on chest radiographs (1). Many investigators have evaluated regional lung ventilation using X-ray fluoroscopy. However, this method has not been adopted for clinical use because of technical limitations (2-8). There have also been many reports of the feasibility of pulmonary densitometry, but this technique has not seen widespread adoption due to the need for special instrumentation, limited field of view, and image distortion (9-10). Dynamic flat-panel detectors (FPD) can provide sequential radiographs with a large field of view and high image quality (11). Dynamic FPD will be used more widely in the near future and overcomes the above difficulties. Moreover, computerized analysis of the digital images obtained would allow real-time quantitative assessment. Therefore, we focused on kinetic imaging using a dynamic FPD, and developed computerized methods for quantifying and visualizing respiratory kinetics, such as diaphragmatic movement and regional lung ventilation (12-15). The results of a preliminary clinical study indicated the clinical usefulness of our method in some pulmonary diseases: in emphysema patients, areas with trapped air were indicated as areas with decreased respiratory changes in pixel values. Although this method is inferior to dynamic magnetic resonance imaging (MRI) and computed tomography (CT) because of the lack of 3D anatomical information, it can be used as a rapid and simple substitute for quantitative assessment of diaphragmatic movement and regional ventilation with dynamic MRI (16-31) and CT (32-35). However, the ability of our method to detect local ventilation remains to be resolved. The present study was performed to investigate the ability of breathing chest radiography using a dynamic FPD to detect ventilation and regional differences in ventilation. In particular, we examined spatial and temporal changes in pixel values on dynamic chest radiographs, and clarified their mechanism according to respiratory physiology as described below.

Respiratory physiology

Local changes in X-ray translucency during respiration are dependent on relative increases and decreases in air and lung vessel volume per unit volume (1). Thus, it may be possible to evaluate relative ventilation quantitatively from respiratory changes in X-ray translucency on dynamic chest radiographs. It is well known that there are regional differences in ventilation in respiratory physiology (36). As described in ref. 36, ventilation per unit volume is greatest near the bottom of the lung and becomes

progressively smaller toward the top. This is because of differences in pressure on local lung area due to the weight of the lung itself. Other measurements showed that when the subject is in the decubitus position (lying on their side), this difference disappears and apical and basal ventilation become equivalent. However, in this posture, ventilation of the dependent lung exceeds that of the upper area. On the other hand, at the end of expiration, the lower airway closes earlier than the upper airway due to the differences in air pressure of the thoracic cavity, *i.e.*, airway closure, and the ventilation in the upper area becomes greater than that in the lower area. The lung volume when airway closure occurs is defined as the "closing volume," which is a very effective index for diagnosing pulmonary diseases. For example, in subjects with chronic obstructive pulmonary disease (COPD) and restrictive pulmonary disease, airway closure appears in early expiratory phase, and as a result closing volume becomes large.

MATERIALS AND METHODS

Image acquisition

Dynamic chest radiographs of six normal subjects (21-52 years old male; mean, 23 years old) were obtained during respiration using a modified FPD system (CXDI-40G, Canon Inc., Tokyo, Japan), X-ray device (KXO 80G, Toshiba, Tokyo, Japan), and X-ray tube (DRX 2724HD 0.6/1.2, Toshiba). Imaging was performed in three different positions (standing, and right and left decubitus positions) (Fig. 1), to change the distribution of local ventilation by changing the pressure caused by the lung's own weight in each area. The subjects had no underlying asthma or smoking history, and an experienced radiologist confirmed that their chest radiographs were normal. In addition, the results of a pulmonary function test also showed that they were normal. The subjects were instructed to respire according to an automated voice to maintain reproducibility and ensure that both respiratory phases were included in the images. The automated voice system instructed the subjects to perform expiration for 5 seconds from maximum inspiration and inspiration for 5 seconds from maximum expiration. The subjects practiced the method of respiration several times before imaging.

The modified FPD was an indirect type made of GOS (Gd^2O^2S (Tb)), and was capable of taking images at up to 6 frames per second. Exposure conditions were 110 kV, 80 mA, 6.3 ms, SID 2 m, 3 frames per second, 2 mm Al filter. The entrance surface dose for 30 frames, measured in air without backscattering, was approximately 0.4 mGy, which was 1.5-fold greater than that of conventional posterioranterior (PA) chest radiography using a Fuji Computed Radiography system (Fuji Medical Systems Co., Ltd., Tokyo, Japan) in our hospital. The matrix size was 1344×1344 pixels, the pixel size was

320×320 μm, and the gray-level range of the images was 4096. Approval for the study was obtained from our institutional review board before beginning any research involving human subjects or clinical information, and the subjects gave their written informed consent to participation.

Low pixel values were related to dark areas in the images, and this in turn was related to high X-ray translucency in this system. The pixel value was inversely proportional to the logarithm of the incident exposure into the FPD as below;

$$(1/P) \propto \log(E) \propto E \propto X \qquad (1)$$

P: pixel value

E: Entrance dose to the detector

X: X-ray translucency of subject

Although this study was performed to measure X-ray translucency, we measured pixel value for ease of handling.

Image Analysis

(a) Preprocessing

Image analysis was performed on a personal computer (Operating system, Windows 2000, Microsoft, Redmond, WA, USA; CPU, Pentium 4, 2.6 GHz; Memory, 1 GB) with our algorithm described below (Development environment: C++Builder; Borland, Scotts Valley, CA, USA).

The lung area was determined by edge detection using the first derivative technique and an iterative contour-smoothing algorithm (37,38). The distance from the lung apex to the diaphragm (abbr. DLD) was measured by the edge detection technique for use as an index of respiratory phase. The point for measurement was the uppermost point of the lung to one point of the diaphragm dome, determined as the midpoint between the mediastinum and rib cage, as shown in Fig. 1(14). The locations of the mediastinum and rib cage were determined based on the midpoint of the length of the longer lung. We then investigated the extents to which the respiratory physiology described in the "Introduction" was reflected in dynamic chest radiographs.

(b) Evaluation of the Ability of our Method to Detect Ventilation

To examine the ability of our method to detect ventilation, we investigated the relationship between pixel value in each lung and DLD, *i.e.*, respiratory phase. We measured average pixel values in each lung and calculated correlation coefficients and

regression lines between the inter-frame differences of the average pixel value (D-frame) and the inter-frame differences of DLD. Statistical significance of the difference between correlation coefficients in each lung was then compared in each position by Student's *t*-test. Differences in regression slopes were also compared in each lung. To examine whether our method could quantify relative inspiratory capacity (IC) of each lung during one respiratory cycle, difference values of the average pixel value between maximum inspiratory and expiratory phase (D-max) were also calculated, and the significance of differences in both lungs was evaluated by Student's *t*-test. The ratios of D-max in the right lung to that in the left lung were also calculated based on D-max of the right lung in the PA standing position. Subsequently, to examine the ability of our system to detect relative ventilation of each lung at the instance and timing of airway closure per lung unit, D-frames of each lung were compared in both lungs by subtracting the absolute D-frame of one lung from that of the other. Definitions of D-max and D-frame are given in (2) and in Fig. 2.

$$D\text{-}\max = P_{MIP} - P_{MEP}$$

$$D\text{-}\,frame(n) = P_n - P_{(n-1)} \quad (1 < n \le 30) \qquad (2)$$

P : *average pixel value*
MIP : *Maximum Inspiratory Phase*
MEP : *Maximum Expiratory Phase*

(c) Evaluation of the Ability of our Method to Detect Regional Differences in Ventilation

To examine the ability of our method to detect regional differences in ventilation, the recognized lung areas were divided equally into horizontal zones throughout all frames as shown in Fig. 3 and Fig. 4, and the average pixel values of each zone were then calculated. The horizontal or vertical division into relatively large areas was used to reduce the influence of differences in rib content and displacement in each area, and to easily compare the measured average pixel values with regional differences in ventilation, which varies significantly in the vertical direction more than horizontal direction. D-max in each zone was also calculated, and the trend of distribution was evaluated by two-way analysis of variance in six normal subjects to test the null

hypothesis that there were no differences in D-max in each zone. Furthermore, to examine the ability of our method to detect the timing of airway closure in each local area, D-frames of each zone as shown in Fig. 3 were calculated, and they were visualized on dynamic chest radiographs in the form of color display according to the magnitude of the D-frame. The color display used a color table in which negative changes (X-ray translucency ↑) were shown in warm colors and positive changes (X-ray translucency ↓) were shown in cold colors.

RESULTS

The Ability of our Method to Detect Ventilation

Figure 5 shows the DLD, measured average pixel values, and D-frame in each lung on dynamic chest radiographs in a normal subject. The inter-frame variation measured in the area without respiratory influence was less than 0.2 %. In all subjects, the average pixel value increased (X-ray translucency ↓) during expiration and decreased (X-ray translucency ↑) during inspiration, and the D-frame showed an inverse correlation with inter-frame difference of DLD at all positions examined (Table 1 and Fig. 6). As shown in Table 1, the correlation coefficient in the dependent lung was greater than that in the non-dependent lung in the decubitus position ($P<0.05$), and there were no significant differences in the standing position. There were no significant differences in regression slopes between the lungs in any position, as shown in Fig. 6. The ratios of average D-max of the right lung to that of the left lung in six subjects, calculated based on D-max of the right lung in the PA standing position, were 0.8:2.0 in the left decubitus position, 1.9:0.7 in the right decubitus position, and 1:1 in the PA standing position. D-max in the dependent lung was larger than that in the non-dependent lung ($P<0.01$) in the decubitus positions, and there were no significant differences between the lungs in the standing position (N.S.). Figure 7 shows the differences in absolute D-frame in both lungs. In the standing position, D-frames of both lungs were similar throughout all respiratory phases. In contrast, in the right and left decubitus positions, D-frames of the dependent lung were larger than those of the non-dependent lung in almost all phases, except at the end of the expiratory phase.

The Ability of our Method to Detect Regional Differences in Ventilation

Figures 8-9 show D-max in the recognized lung area divided into eight zones in all positions. D-max in each zone indicated the following tendencies in each position. In the standing position, D-max in the lower zone was greater than that in the upper zone ($P<0.01$), and D-max in the thoracic cage side was greater than that in the mediastinum

side ($P<0.01$) (Fig. 8a and 9a). In both left and right decubitus positions, D-max in the lower zone was greater than that in the upper zone ($P<0.01$) (Fig. 8b). There were no significant differences between the upper and lower lung fields in the non-dependent lung. However, in the dependent lung, a significant difference was observed between the upper and lower lung fields ($P<0.01$) (Fig. 9b).

Dynamic chest radiographs superimposed with D-frame in each horizontal zone are shown in Figs. 10–11. Warm colored areas show negative changes in pixel value (X-ray translucency ↑), cold colored areas show positive changes in pixel value (X-ray translucency ↓), and colorless areas show no or little changes in pixel value. The changes in pixel values are expressed by saturation as shown in the color table superimposed in Fig. 10–11. Thus, images in inspiratory phase were mainly warm colors, whereas images in expiratory phase were mainly cold colors. Images in the maximum inspiratory or expiratory phase showed little or no color. In all positions, lower zones are expressed as the area with a large change in almost all phases. However, in both decubitus positions, the horizontal zones where there were large D-frames, shown in deep blue, moved up in the vertical direction during expiration. All six subjects showed the same patterns.

DISCUSSION

In evaluation of the ability of our method to detect ventilation, the average pixel value in each lung was associated with the respiratory phase in all normal subjects. The results indicated that relative ventilation of each lung could be measured from the respiratory changes in pixel values on dynamic chest radiographs. In the decubitus position, correlation coefficients of the dependent lung were greater than those of the non-dependent lung. This was explained because the diaphragm overwhelmingly contributes to respiration more than the intercostals muscles, due to limited rib cage movement in the dependent lung.

D-max of the dependent lung was significantly greater than that of the non-dependent lung in the decubitus positions. Although the differences were not statistically significant, the regression slope, *i.e.*, the respiratory changes in pixel values per diaphragmatic movement, in the dependent lung were slightly larger than those in the non-dependent lung in the decubitus position. This was considered due to differences in the location of the lung, *i.e.*, gravitational influence, because there were no significant differences in the standing position. The results were consistent with well-known properties in respiratory physiology, in which ventilation is known to be greater in the upper area than in the lower area. Thus, the relative values in each lung,

i.e., the ratio of IC in the right lung to that in the left lung, could be quantified from D-max on dynamic chest radiographs.

The time when D-frame in the non-dependent lung was greater than that in the dependent lung, as seen at the end of expiration in Fig. 7(a) and (c), indicated the advantage of ventilation in the non-dependent lung. The results indicated that our method was capable of quantifying instantaneous relative ventilation in each lung and detecting airway closure per lung unit.

In evaluation of regional differences in ventilation, D-max in each horizontal zone showed the same tendency as the regional differences in ventilation determined by respiratory physiology. These results indicated that our method was capable of detecting regional differences in ventilation. However, in both lungs in the standing position and in the non-dependent lung in the decubitus positions, D-max in each vertical zone showed a tendency that was contrary to the rule "ventilation in the lower area is greater than that in the upper area." The primary reason for this was thought to be because these areas contained a large proportion of the lower area. Another reason was that these areas were strongly influenced by the disappearance and reappearance of a portion of the lung during respiration, resulting from the large range of diaphragmatic movement.

On the other hand, the D-frame in each zone reached their maximum values in the lower-first direction, *i.e.*, from the lower to the upper area, in expiratory phase in decubitus positions. These results indicated that our method can detect airway closure in the local lung area. However, there were some unexpected results that were contrary to respiratory physiology in the standing position, in which D-frames were negative despite the expiratory phase in the upper zones. Thus, it was difficult to recognize airway closure in the standing position. These results were due to the measurement accuracy of our method. As the directions of measurement zones were perpendicular to the direction of diaphragmatic movement, our method cannot measure average pixel values at the same level of the vertical direction during respiration. In addition, the measured results may be influenced by the degree of rib shadows, because the measurement zones were horizontal to the ribs unlike in the decubitus positions. Thus, it is necessary to develop the method for measuring pixel values in the same location throughout the lungs during respiration. In the abnormal cases, abnormal opacities could have some impact on the measurements. Non-geometric image deformation and measurement in pixel units could be the answer to these problems.

In our previous study, it was shown that the changes in pixel value in the lung had strong association with respiratory phase (13). In the present study, our method was

shown to be capable of measuring spatial and temporal changes of regional relative ventilation. The next step is to investigate normalization of the data among subjects and the pattern model of the normal lungs. Furthermore, it is necessary to correlate respiratory changes in pixel value with a quantitative number, which directly leads to clinical condition. However, it would be difficult to define as CT value, because a volume of lung tissues contribute to each pixel. In the present method, it would be more effective for the diagnosis of pulmonary diseases to compare the results in both lungs or evaluate the distribution. On the other hand, in our ongoing study in combination with an electrocardiogram recorder, the impact of cardiac motion was identified to be less than 10% against the respiratory changes in pixel value. Although it is not considered to have a significant impact on quantification of lung ventilation, it is also necessary to develop a method for noise rejection resulting from cardiac motion.

The main merit of our dynamic study is that it can be used to evaluate the function of each lung separately and that the images can be used to analyze the process of change from inspiration to expiration and *vice versa*. It should be noted that the dose absorbed with our method is up to 1.5-fold that associated with conventional PA chest radiography using an FCR system employed at our hospital. The present method has the potential of becoming widely and conventionally used for analyzing regional lung ventilation because FPD will be more widely used in the near future. Although the present method is inferior to the MRI method because of the lack of 3D anatomic information and the presence of radiation exposure for patients, it can be utilized as a conventional and likely quick method in the evaluation of regional lung ventilation. Furthermore, our computer algorithm can be applied to future diagnostic modalities such as 4D CT.

The main target diseases of our method are COPD and acute pulmonary diseases. Patients with COPD take time to expire, and also ventilate insufficiently due to trapped air. Using our method, it would be possible to detect abnormalities, such as decreases in D-max or D-frame and the early appearance of airway closure at the expiratory phase, in patients with COPD.

CONCLUSION

Breathing chest radiography using an FPD combined with our computerized methods was shown to be capable of quantifying relative ventilation in local lung area, and detecting regional differences in ventilation. In addition, it was suggested that our method could detect airway closure occurring at the end of expiration. Although the present method lacks 3D anatomic information, it is expected to be utilized as a

conventional and quick method in the evaluation of regional lung ventilation. Furthermore, our computer algorithm can be applied to future diagnostic modalities such as 4D CT.

ACKNOWLEGMENTS

This work was supported in part by Canon Inc. and a Grant-in-Aid for Scientific Research from the Japanese Ministry of Education, Culture, Sports, Science, and Technology. The authors are grateful to Hitoshi Inoue at Canon Inc., and the staff of the Dept. of Radiology, Kanazawa University Hospital, who assisted with data acquisition. We thank Katsumi Inoue at Kanazawa University for valuable discussions regarding statistical analysis.

REFERENCES

1. Squire LF and Novelline RA: Overexpansion and collapse of the lung. In: Fundamentals of radiology, 4th ed. Cambridge, Massachusetts, and London, England: Harvard University Press, 88-89, 1988

2. Toffolo RR, Beerel FR: The autofluoroscope and 133-Xe in dynamic studies of pulmonary perfusion and ventilation. Radiology94:692-696, 1970

3. George RB, Weill H, Tahir AH: Fluorodensimetric evaluation of regional ventilation in chronic obstructive pulmonary disease. South Med J.64:1161-1165, 1971

4. George RB, Weill H. Fluorodensimetry. A method for analyzing regional ventilation and diaphragm function. JAMA 217:171-176, 1971

5. Silverman NR: Clinical video-densitometry. Pulmonary ventilation analysis. Radiology 103:263-265, 1972

6. Desprechins B, Luypaert R, Delree M, Delree M, Freson M, Malfroo A, Dab I, Piesz A: Evaluation of time interval difference digital subtraction fluoroscopy patients with cystic fibrosis. Scand J Gastroenterol Suppl 143:86-92, 1988

7. Lam KL, Chan HP, MacMahon H, Oravecz WT, Doi K: Dynamic digital subtraction evaluation of regional pulmonary ventilation with nonradioactive xenon. Invest. Radiol. 25:728-735, 1990

8. Kiura A, Svedstrom E, Kuuluvainen I: Dynamic imaging of pulmonary ventilation. Description of a novel digital fluoroscopic system. Acta Radiol 32:114-119, 1991

9. Baily NA: Video techniques for x-ray imaging and data extraction from roentgenographic and fluoroscopic presentations. Med Phys 7:472-491, 1980

10. Fujita H, Doi K, MacMahon H, Kume Y, Giger ML, Hoffmann KR: Basic imaging properties of a large image intensifier-TV digital chest radiographic system. Invest Radiol 22:328-335, 1987

11. Vano E, Geiger B, Schreiner A, Back C, Beissel J: Dynamic flat panel detector versus image intensifier in cardiac imaging: dose and image quality. Phys Med Biol 50:5731-42, 2005

12. Tanaka R, Sanada S, Suzuki M, Kobayashi T, Matsui T, Inoue H: Automated analysis for the respiratory kinetics with the screening dynamic chest radiography using a flat-panel detector system. Proceedings of 17th International Congress and Exhibition; 2003 June 25-28; London, UK: Computer Assisted Radiology and Surgery, 179-186, 2003

13. Tanaka R, Sanada S, Suzuki M, Kobayashi T, Matsui T, Inoue H, Nakano H: Breathing chest radiography using a dynamic flat-panel detector (FPD) combined with computer analysis. Med Phys 31:2254-2262, 2004

14. Tanaka R, Sanada S, Kobayashi T, Suzuki M. Matsui T, Matsui O. Computerized methods for determining respiratory phase on dynamic chest radiographs obtained by a dynamic flat-panel detector (FPD) system. J Digital Imag 19:41-51, 2006
15. Tanaka R, Sanada S, Okazaki N, Kobayashi T, Fujimura M, Yasui M, Matsui T, Nakayama K, Nanbu Y, Matsui O: Evaluation of pulmonary function using breathing chest radiography with a dynamic flat-panel detector (FPD): Primary results in pulmonary diseases. Invest Radiol, 41:735-745, 2006.
16. Suga K, Tsukuda T, Awaya H, Takano K, Koike S, Matsunaga N, Sugi K, Esato K: Impaired respiratory mechanics in pulmonary emphysema: evaluation with dynamic breathing MRI. J. Magn Reson Imaging 10:510-520, 1999
17. Berthezene Y, Croisille P, Wiart M, Howarth N, Houzard C, Faure O, Douek P, Amiel M, Revel D: Prospective comparison of MR lung perfusion and lung scintigraphy. J Magn Reson Imagig 9:61-68, 1999
18. Maki DD, Gefter WB, and Alavi A: Recent advances in pulmonary imaging. Chest 116:1388-1402, 1999
19. Hatabu H, Chen Q, Stock KW, Gefter WB, Itoh H: Fast magnetic resonance imaging of the lung. Eur J Radiol 29:114-132, 1999
20. Unal O, Arslan H, Uzun K, Ozbay B, Sakarya ME: Evaluation of diaphragmatic movement with MR fluoroscopy in chronic obstructive pulmonary disease. Clin Imaging 24:347-350, 2000
21. Suga K, Tsukuda T, AwayaH, Matsunaga N, Sugi K, Esato K: Interactions of regional respiratory mechanics and pulmonary ventilatory impairment in pulmonary emphysema: assessment with dynamic MRI and xenon-133 single-photon emission CT. Chest 117:1646-1655, 2000
22. Amundsen T, Torheim G, Waage A, Bjermer L, Steen PA, Haraldseth O: Perfusion magnetic resonance imaging of the lung: characterization of pneumonia and chronic obstructive pulmonary disease. A feasibility study. J Magn Reson Imaging 12:224-231, 2000
23. Kauczor HU, Kreitner KF. Contrast-enhanced MRI of the lung. Eur J Radiol 34:196-207, 2000
24. Cluzel P, Similowski T, Chartrand-Lefebvre C, Zelter M, Derenne JP, Grenier PA: Diaphragm and chest wall: assessment of the inspiratory pump with MR imaging-preliminary observations. Radiology 215:574-583, 2000
25. Salerno M, Altes TA, Mugler JP 3rd, Nakatsu M, Hatabu H, de Lange EE: Hyperpolarized noble gas MR imaging of the lung: potential clinical applications. Eur J Radiol 40:33-44, 2001

26. Kauczor HU, Chen XJ, van Beek EJ, Schreiber WG: Pulmonary ventilation imaged by magnetic resonance: at the doorstep of clinical application. Eur Respir J 17:1008-1023, 2001
27. Ohno Y, Hatabu H, Takenaka D, Van Cauteren M, Fujii M, Sugimura K: Dynamic oxygen-enhanced MRI reflects diffusing capacity of the lung. Magn Reson Med 47:1139-1144, 2002
28. Kauczor HU, Hanke A, Van Beek EJ. Assessment of lung ventilation by MR imaging: current status and future perspectives. Eur Radiol 12:1962-1970, 2002
29. Kotani T, Minami S, Takahashi K. Isobe K, Nakata Y, Takaso M, Inoue M, Maruta T, Akazawa T, Ueda T, Moriya H: An analysis of chest wall and diaphragm motions in patients with idiopathic scoliosis using dynamic breathing MRI. Spine 29:298-302, 2004
30. Van Beek EJ, Wild JM, Kauczor HU, Schreiber W, Mugler JP 3rd, de Lange EE: Functional MRI of the lung using hyperpolarized 3-helium gas. J Magn Reson Imaging 20:540-554, 2004
31. Haage P, Karaagac S, Spuntrup E, Truong HT, Schmidt T, Gunther RW: Feasibility of pulmonary ventilation visualization with aerosolized magnetic resonance contrast media. Invest Radiol 40:85-88, 2005
32. Webb WR, Stern JE, Kanth N, Gamsu G: Dynamic Pulmonary CT: Findings in healthy adult men. Radiology 186:117-124, 1993
33. David M, Athol U, Michael B, Peter J: Bronchiectasis: Functional significance of areas of decreased attenuation at expiratory CT. Radiology 193:369-374, 1994
34. Johnson JL, Kramer SS, Mahboubi S. Air trapping in children: evaluation with dynamic lung densitometry with spiral CT. Radiology 206:95-101, 1998
35. Bakker ME, Stolk J, Putter H, Shaker SB, Parr DG, Piitulainen E, Russi EW, Dirksen A, Stockley RA, Reiber JH, Stoel BC: Variability in densitometric assessment of pulmonary emphysema with computed tomography. Invest Radiol 40:777-783, 2005
36. West JB. Ventilation – how gas gets to the alveoli. In: Respiratory physiology – the essentials 6th ed. Philadelphia, PA: Lippincott Williams & Wilkinss, 11-19, 2000
37. Xu XW, Doi K: Image feature analysis for computer-aided diagnosis: accurate determination of ribcage boundary in chest radiographs. Med Phys 22:617-626, 1995
38. Li L, Zheng Y, Kallergi M, Clark RA: Improved method for automatic identification of lung regions on chest radiographs. Acad Radiol 8:629-638, 2001

Legends

Fig. 1 Dynamic chest radiographs obtained by our FPD system

(a) Left decubitus position. (b) PA standing position. (c) Right decubitus position. (Normal subject, 24M). The arrows show the points for measuring the distance from the lung apex to the diaphragm.

Fig. 2 Definitions of D-max and D-frame. D-max is the maximum change in average pixel value during one respiratory phase. D-frame is the change in average pixel value at the instant.

MIP: Maximum Inspiratory Phase, MEP: Maximum Expiratory Phase, D-max: Difference values of the average pixel value between MIP and MEP, D-frame: Inter-frame differences of the average pixel value

Fig. 3 Dynamic chest radiographs were divided horizontally into eight zones per lung. (a) Left decubitus position. (b) PA standing position. (c) Right decubitus position.

Fig. 4 Dynamic chest radiographs were divided vertically into eight zones per lung. (a) Left decubitus position. (b) PA standing position. (c) Right decubitus position.

Fig. 5 DLD, average pixel values, and D-frame in each lung during respiration in (a) left decubitus position, (b) PA standing position, and (c) right decubitus position. (Normal subject, 24M). In the maximum inspiration and expiration, standard deviations in the subjects of DLD were 1.7 cm and 2.5 cm, respectively. The average pixel values showed standard deviations of 134.2 and 153.1, respectively.

DLD: Distance from lung apex to the diaphragm, D-frame: Inter-frame differences of the average pixel value

Fig. 6 Relationship between inter-frame differences in DLD and D-frame in each lung, in (a) left decubitus position, (b) PA standing position, and (c) right decubitus position, in all subjects. (n=180; 30 points per subject).

D-frame: Inter-frame differences of the average pixel value, DLD: Distance from lung apex to the diaphragm

Fig. 7 Differences in absolute D-frame in both lungs in (a) left decubitus position, (b) PA standing position, and (c) right decubitus position, which was derived by taking the absolute D-frame in the non-dependent lung from that in the dependent lung. (Normal subject, 24M).

D-frame: Inter-frame differences of the average pixel value

Fig. 8 D-max in the recognized lung area divided into eight zones in the vertical direction. The values are averages of six normal subjects in (a) standing position and (b) right and left decubitus positions.

D-max: Difference values of the average pixel value between maximum inspiratory and

expiratory phase

Fig. 9 D-max in the recognized lung area divided into eight zones in the horizontal direction. The values are averages of six normal subjects in (a) standing position and (b) right and left decubitus positions.

D-max: Difference values of the average pixel value between maximum inspiratory and expiratory phase

Fig. 10 Dynamic chest radiographs in the left decubitus position superimposed with D-frame in each zone in color display, and DLD as an index of respiratory phase. (Normal subject, 24M).

D-frame: Inter-frame differences of the average pixel value, DLD: Distance from lung apex to the diaphragm

Fig. 11 Dynamic chest radiographs in the PA standing position superimposed with D-frame in each zone in color display, and DLD as an index of respiratory phase. (Normal subject, 24M).

D-frame: Inter-frame differences of the average pixel value, DLD: Distance from lung apex to the diaphragm

Table 1 Correlation coefficient between D-frame and inter-frame differences in DLD in each lung.

N.S.: Not significant

D-frame: Inter-frame differences of the average pixel value, DLD: Distance from lung apex to the diaphragm

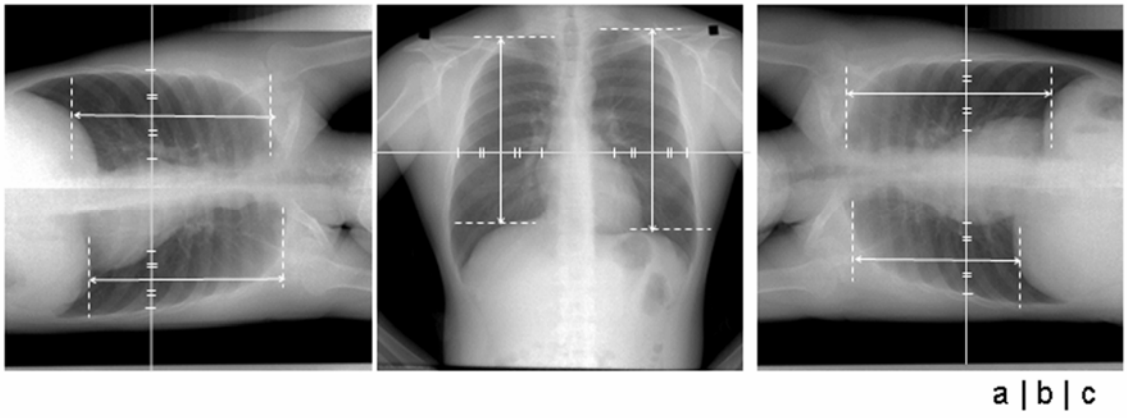

Fig. 1 Dynamic chest radiographs obtained by our FPD system
(a) Left decubitus position. (b) PA standing position. (c) Right decubitus position. (Normal subject, 24M). The arrows show the points for measuring the distance from the lung apex to the diaphragm.

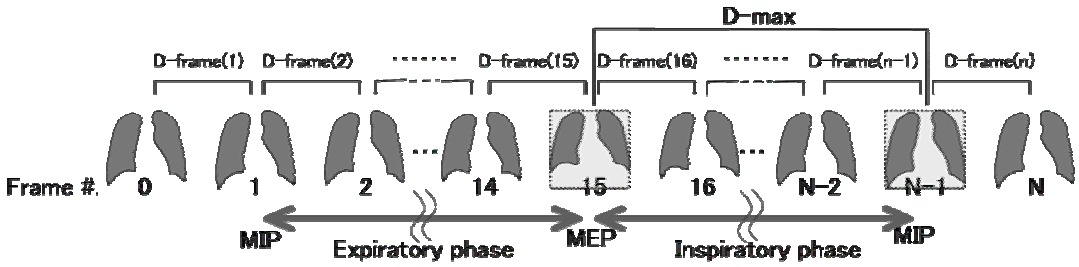

Fig. 2 Definitions of D-max and D-frame. D-max is the maximum change in average pixel value during one respiratory phase. D-frame is the change in average pixel value at the instant.
MIP: Maximum Inspiratory Phase, MEP: Maximum Expiratory Phase, D-max: Difference values of the average pixel value between MIP and MEP, D-frame: Inter-frame differences of the average pixel value

Fig. 3 Dynamic chest radiographs were divided horizontally into eight zones per lung. (a) Left decubitus position. (b) PA standing position. (c) Right decubitus position.

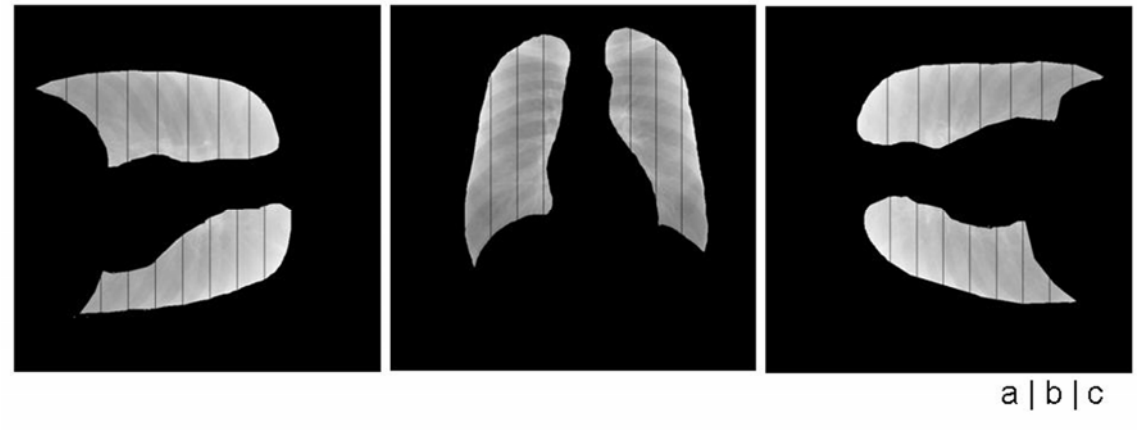

Fig. 4 Dynamic chest radiographs were divided vertically into eight zones per lung. (a) Left decubitus position. (b) PA standing position. (c) Right decubitus position.

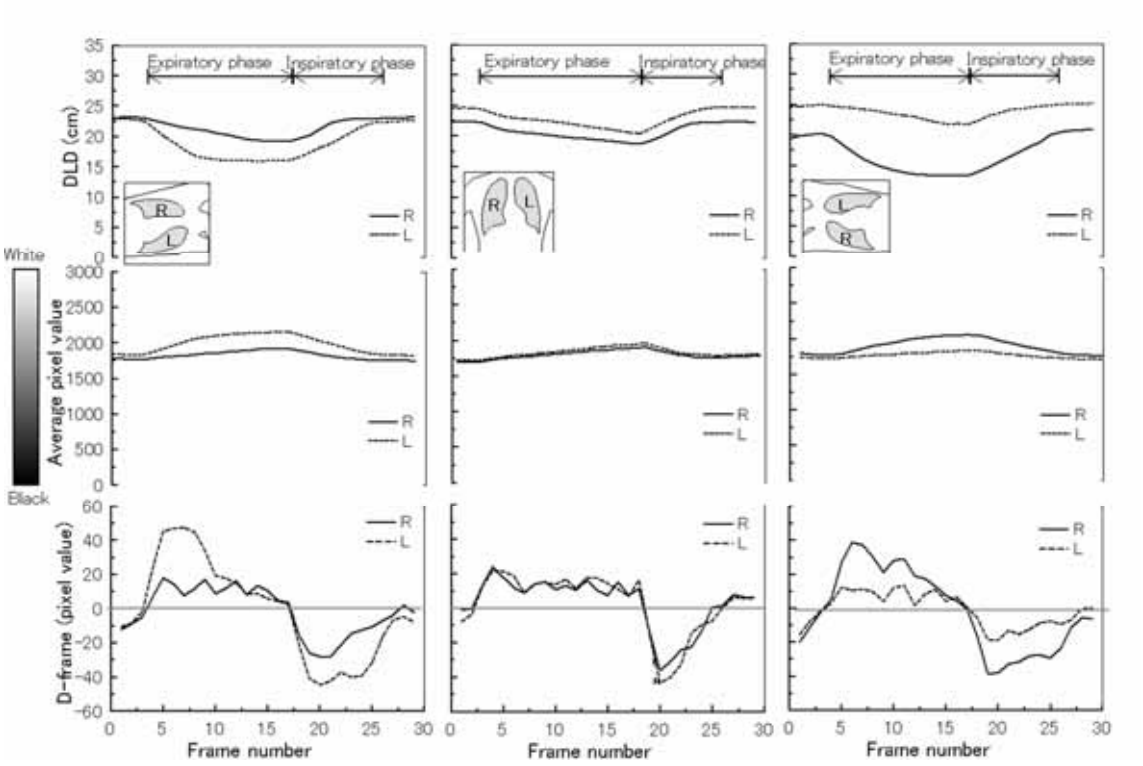

Fig. 5 DLD, average pixel values, and D-frame in each lung during respiration in (a) left decubitus position, (b) PA standing position, and (c) right decubitus position. (Normal subject, 24M). In the maximum inspiration and expiration, standard deviations in the subjects of DLD were 1.7 cm and 2.5 cm, respectively. The average pixel values showed standard deviations of 134.2 and 153.1, respectively.

DLD: Distance from lung apex to the diaphragm, D-frame: Inter-frame differences of the average pixel value

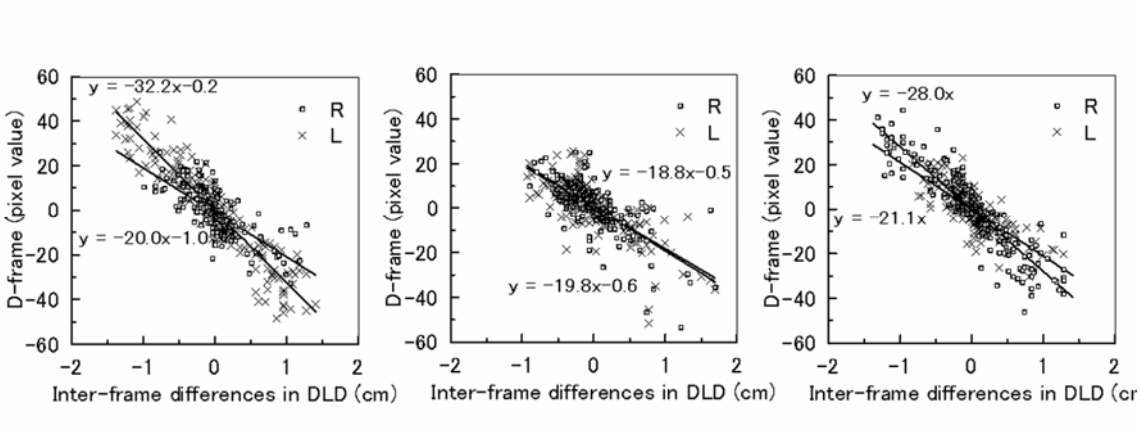

Fig. 6 Relationship between inter-frame differences in DLD and D-frame in each lung, in (a) left decubitus position, (b) PA standing position, and (c) right decubitus position, in all subjects. (n=180; 30 points per subject).

D-frame: Inter-frame differences of the average pixel value, DLD: Distance from lung apex to the diaphragm

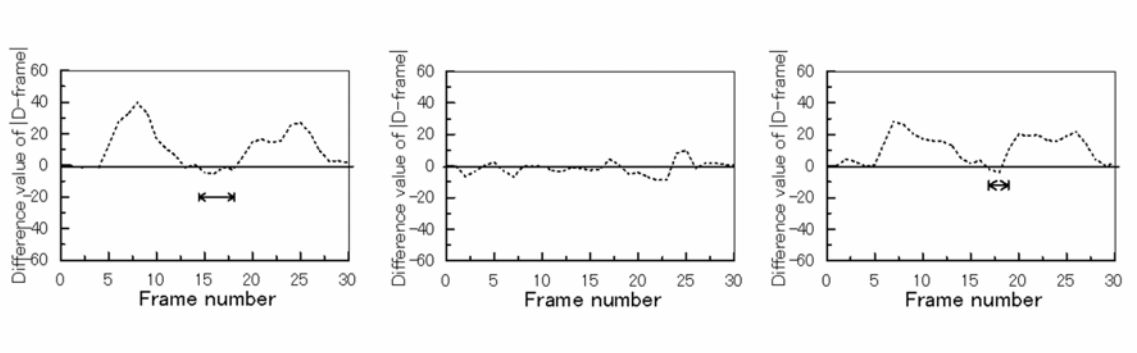

Fig. 7 Differences in absolute D-frame in both lungs in (a) left decubitus position, (b) PA standing position, and (c) right decubitus position, which was derived by taking the absolute D-frame in the non-dependent lung from that in the dependent lung. (Normal subject, 24M).

D-frame: Inter-frame differences of the average pixel value

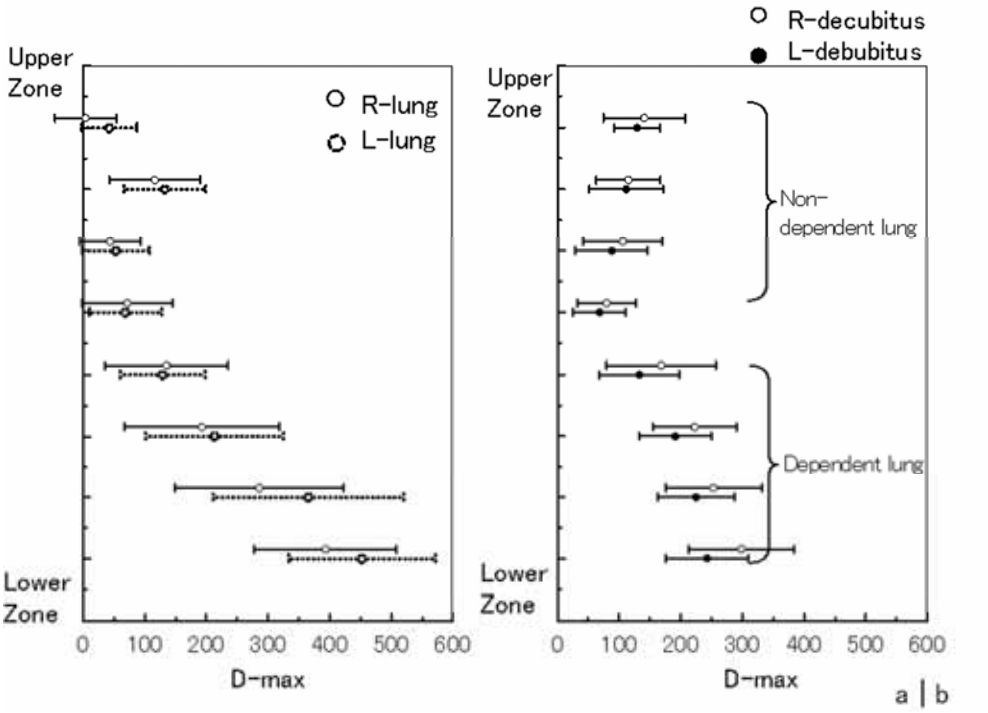

Fig. 8 D-max in the recognized lung area divided into eight zones in the vertical direction. The values are averages of six normal subjects in (a) standing position and (b) right and left decubitus positions.

D-max: Difference values of the average pixel value between maximum inspiratory and expiratory phase

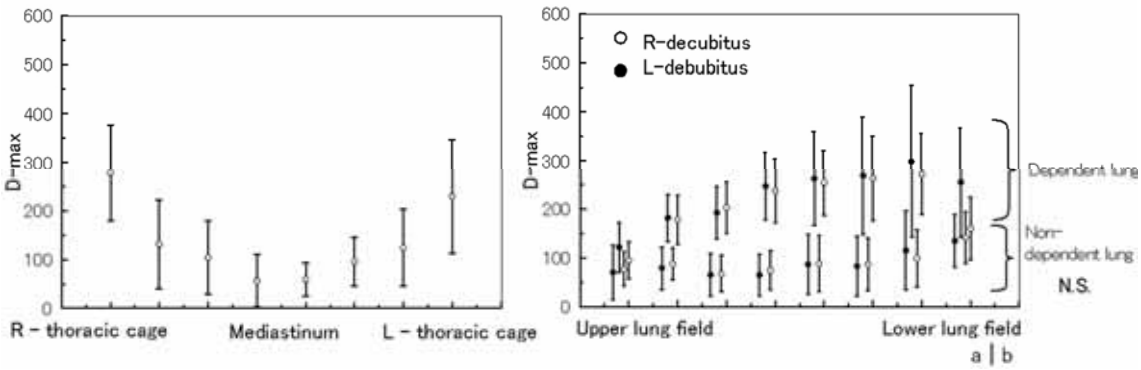

Fig. 9 D-max in the recognized lung area divided into eight zones in the horizontal direction. The values are averages of six normal subjects in (a) standing position and (b) right and left decubitus positions.

D-max: Difference values of the average pixel value between maximum inspiratory and expiratory phase

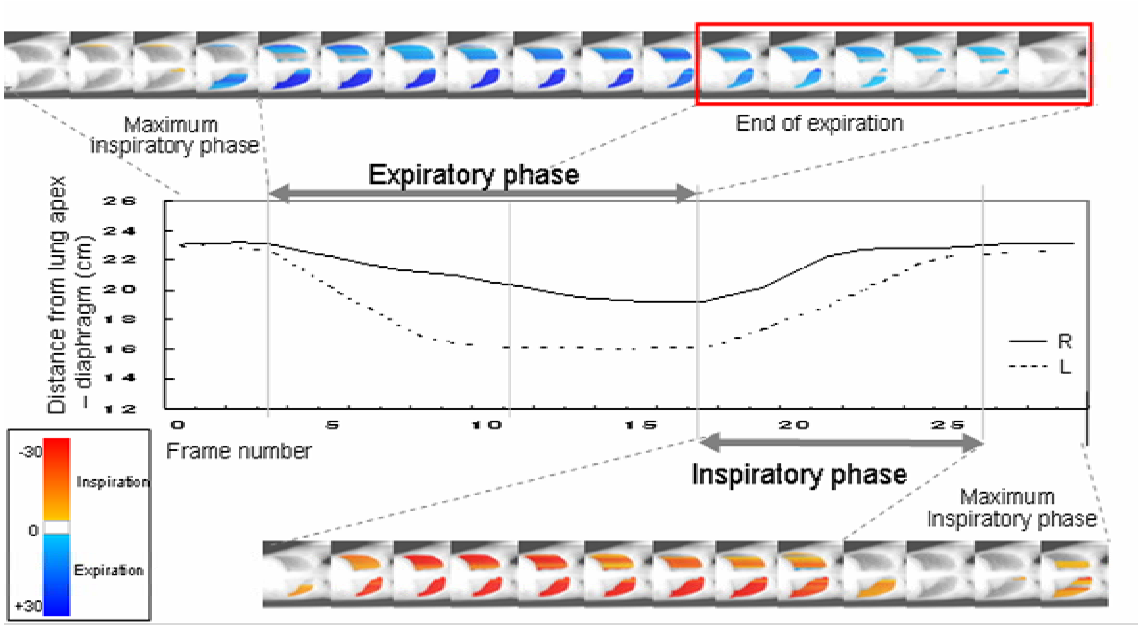

Fig. 10 Dynamic chest radiographs in the left decubitus position superimposed with D-frame in each zone in color display, and DLD as an index of respiratory phase. (Normal subject, 24M).

D-frame: Inter-frame differences of the average pixel value, DLD: Distance from lung apex to the diaphragm

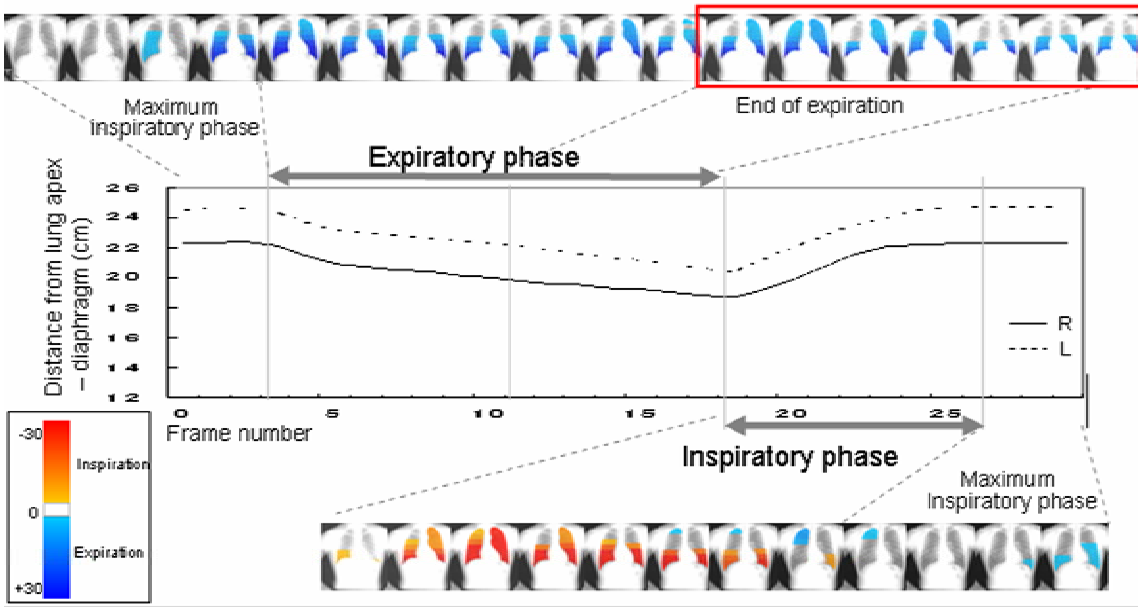

Fig. 11 Dynamic chest radiographs in the PA standing position superimposed with D-frame in each zone in color display, and DLD as an index of respiratory phase. (Normal subject, 24M).

D-frame: Inter-frame differences of the average pixel value, DLD: Distance from lung apex to the diaphragm

Positioning	Lung	Correlation coefficient (r)	Significant difference
Left decubitus position	Right	- 0.72	P<0.05
	Left	- 0.94	
Standing position	Right	- 0.72	N.S.
	Left	- 0.74	
Right decubitus position	Right	- 0.92	P<0.05
	Left	- 0.76	

Table 1 Correlation coefficient between D-frame and inter-frame differences in DLD* in each lung.

N.S.: Not significant

* The distance from the lung apex to the diaphragm